

PFC/JA-90-39

Design Optimization of Ignited Tokamaks

E.A. Chaniotakis

J.P. Freidberg

D.R. Cohn

November 1990

Plasma Fusion Center
Massachusetts Institute of Technology
Cambridge, Massachusetts 02139 USA

This work was supported by the Princeton Plasma Physics Lab under sub-contract No.: S-02969-A.

Design Optimization of Ignited Tokamaks

E.A. Chaniotakis, J.P. Freidberg, D.R. Cohn

Massachusetts Institute of Technology

Abstract

In this paper we write the 0-D energy balance in terms of the parameters $W \equiv \frac{B\tau}{R}$, $N \equiv \frac{nR}{B}$, and $\Pi \equiv \frac{P_a R}{\alpha^2 B^2}$. The minimum value of W required to achieve ohmic ignition (i.e. $\Pi = 0$) in the generic case (i.e. no n or T dependence on τ), and for various dependencies of τ on n and T is $W \sim 15$ in all cases. Also the value of W below which no access, even with the aid of auxiliary power, to high temperature alpha dominated operation is possible is $W \sim 2$ in all cases. Optimized designs are obtained by minimizing the ratio of the auxiliary power p_a to the ohmic power p_Ω at the Cordey pass. The optimization is consistent with the physics requirements, the toroidal field coil volume and stress constraints, and with the volt-second and stress constraints of the ohmic transformer. Results under various τ dependencies are presented.

1 Introduction

The zero dimensional power balance can be written in the compact form.

$$\tau_E \frac{dT}{dt} = -T + W \left[\frac{C_\Omega}{NT^{3/2}} + N (C_\alpha F - C_b T^{1/2}) \right] + C_a \frac{W\Pi}{N} \quad (1)$$

Where, $T(t)$ is the peak temperature, $W \equiv B\tau_E/R$ is a basic parameter measuring machine performance, $N \equiv nR/B$ is a normalized form of the

density, and $\Pi \equiv P_a R/a^2 B^2$ is a normalized form of the total auxiliary power $P_a = \langle p_a \rangle V_p$ where V_p is the plasma volume. The function $F(T)$ and the coefficients C_j are given in Appendix A. In these expressions and all that follow, the units are T (keV), $n(10^{20} \text{ m}^{-3})$, B (T), a (m), R (m), τ_E (sec), and P_a (MW). In summary the quantities W , N , Π are given by

$$W = \frac{B\tau_E}{R} \quad (2)$$

$$N = \frac{nR}{B} \quad (3)$$

$$\Pi = \frac{P_a R}{a^2 B^2} \quad (4)$$

Equation (1) is the power balance relation describing the time evolution of T . There are many ways to rewrite Eq. (1) by defining a different set of parameters. The choices made here for W and N are crucial for a proper understanding of ignition. The critical issue is that n and τ_E are not interchangeable parameters in the design of an ignition experiment. In a given device, $n \sim N$ can be easily varied over a reasonably wide range of parameters without affecting the cost. N is constrained only by a practical experimental operating limit,¹ known as the Murakami [3] limit given by

$$N \leq N_m = 1.4 \quad (5)$$

In contrast, raising $\tau_E \sim W$ invariably requires an increase in either field, current, or machine size and, hence, cost. Consequently, $W = B\tau_E/R$ gives a measure of machine performance and cost. It is more reliable than such traditional parameters as $n\tau_E$ or $n\tau_E T$ which do not distinguish between high n -low τ_E (low cost) or low n -high τ_E (high cost).

¹There is a second operational limit due to MHD instabilities known as the Troyon [1,2] limit, $N < N_\beta = 1.12IR/aT$. In the analysis, the Murakami limit is assumed more severe. The β limit is tested a posteriori, once the final geometry is decided.

In general the energy confinement time τ_E can be written as

$$\tau_E = \mathcal{G}(a, R, \kappa, \dots) \mathcal{F}(N, T, \Pi) \quad (6)$$

where \mathcal{G} is a function of geometry (a, R, κ, \dots) , and \mathcal{F} is a function of temperature, density, and auxiliary power. Therefore, the parameter W may be written as

$$W = \widehat{W} \mathcal{F}(N, T, \Pi) \quad (7)$$

$$\widehat{W} = \frac{B}{R} \mathcal{G}(a, R, \kappa, \dots) \quad (8)$$

In this general case \widehat{W} serves as a performance parameter. In particular the following cases are investigated.

- Generic. $\mathcal{F}(N, T, \Pi) = 1$
 - Ohmic. $\mathcal{F}(N, T, \Pi) = N$
 - Auxiliary1. $\mathcal{F}(N, T, \Pi) = 1/T^{0.5}$
 - Auxiliary2. $\mathcal{F}(N, T, \Pi) = N/T$
- (9)

2 Ignition Definition

The natural definition of ignition follows from an examination of the \dot{T} vs T diagram. Depending upon the size of W there are three qualitatively different regimes to distinguish: ohmic ignition, auxiliary power ignition, and non-ignited operation.

Figure 1 illustrates the most desirable regime of operation. Observe that for $P_a = 0$ there are three steady state equilibrium solutions corresponding to $\dot{T} = 0$. The left point, denoted by T_Ω , represents the temperature achieved in an ohmic discharge $\langle p_\Omega \rangle \approx \langle p_l \rangle$ and is dominated by $1/T^{3/2}$ dependence of the ohmic power term. It typically occurs at $T_\Omega \sim 2 - 3$ keV.

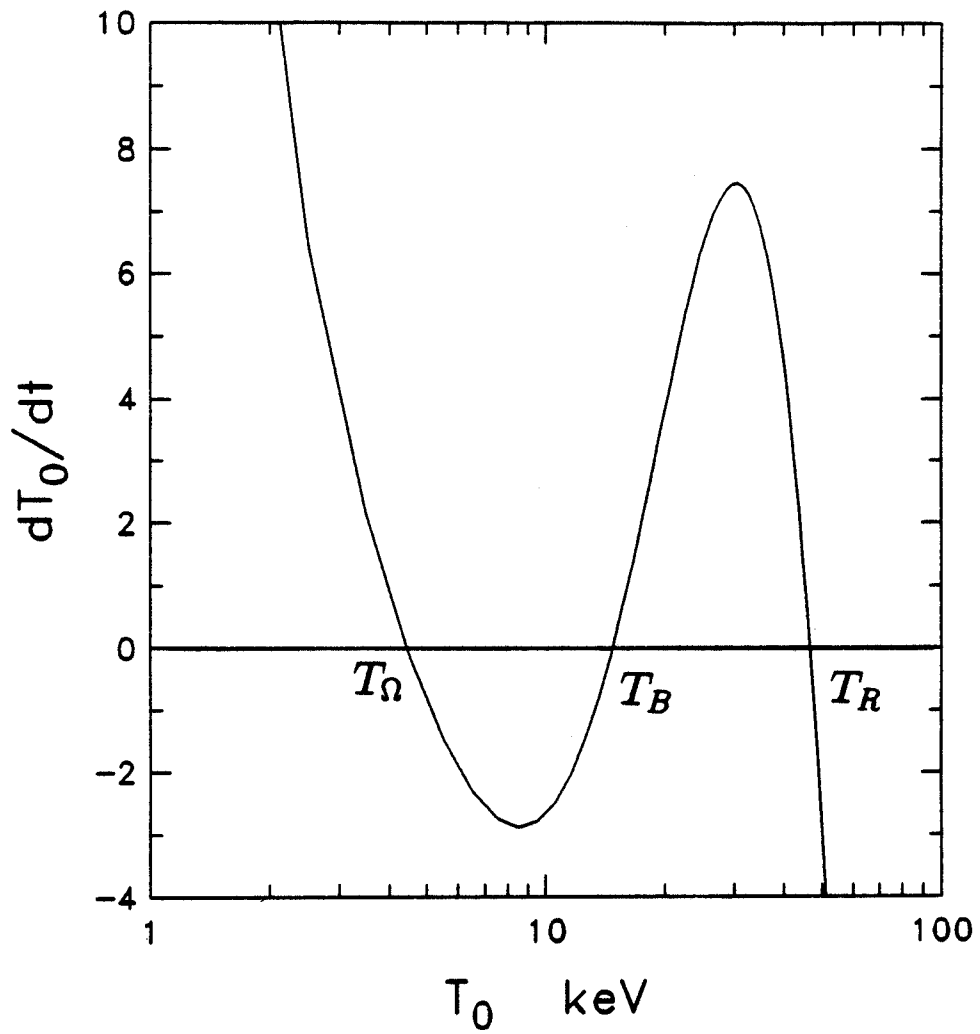


Figure 1: Illustrative \dot{T} vs T plot with the three equilibrium points T_Ω , T_B , and T_R

The second equilibrium point T_B is dominated by alpha particle heating and usually occurs at $T_B \sim 12 - 20$ keV. Since the optimum temperature for fusion power production, at fixed β , occurs at $T \sim 15$ keV this is ultimately the desired operating temperature. The third equilibrium point, T_R , represents the final stable temperature. It typically occurs at $T_R \sim 50$ keV as a consequence of the high temperature decay of the $\bar{\sigma}v$ curve. This point, even though stable, is uninteresting because the plasma β is far above the MHD stability limit and corresponds to operation far from at the optimum temperature for fusion power production.

Unfortunately, it is not possible to gain access to the high temperature equilibrium point T_B through the normal evolution of the ohmic discharge. The reason is as follows. At the initiation of the discharge the temperature is very low and ohmic heating is the dominant mechanism in the power balance relation. As time increases the temperature increases since $\dot{T} > 0$. This is equivalent to moving to the right along the T axis. Once the low temperature ohmic equilibrium point, T_Ω , is reached the temperature can increase no further. Any increase in temperature causes $\dot{T} < 0$ which drives the system back to the ohmic equilibrium point. Stated physically, for temperatures greater than that corresponding to the ohmic point, the losses increase faster than the ohmic power input.

It is thus clear that in order to reach the high temperature regime the value of W or P_a must be sufficiently high so that the minimum of the \dot{T} curve lies above the axis. In this situation, $\dot{T} \geq 0$ during the entire evolution, thereby providing access to the alpha particle dominated operation. The temperature at which the minimum of the \dot{T} curve becomes tangent to the horizontal (T) axis is denoted by T_I , and is called the ignition temperature hereinafter.

There are two ways to achieve $\dot{T} \geq 0$. First, for $P_a = 0$ the minimum of the \dot{T} curve can be raised above the axis by increasing the machine performance (and hence cost); this is equivalent to raising the value of W

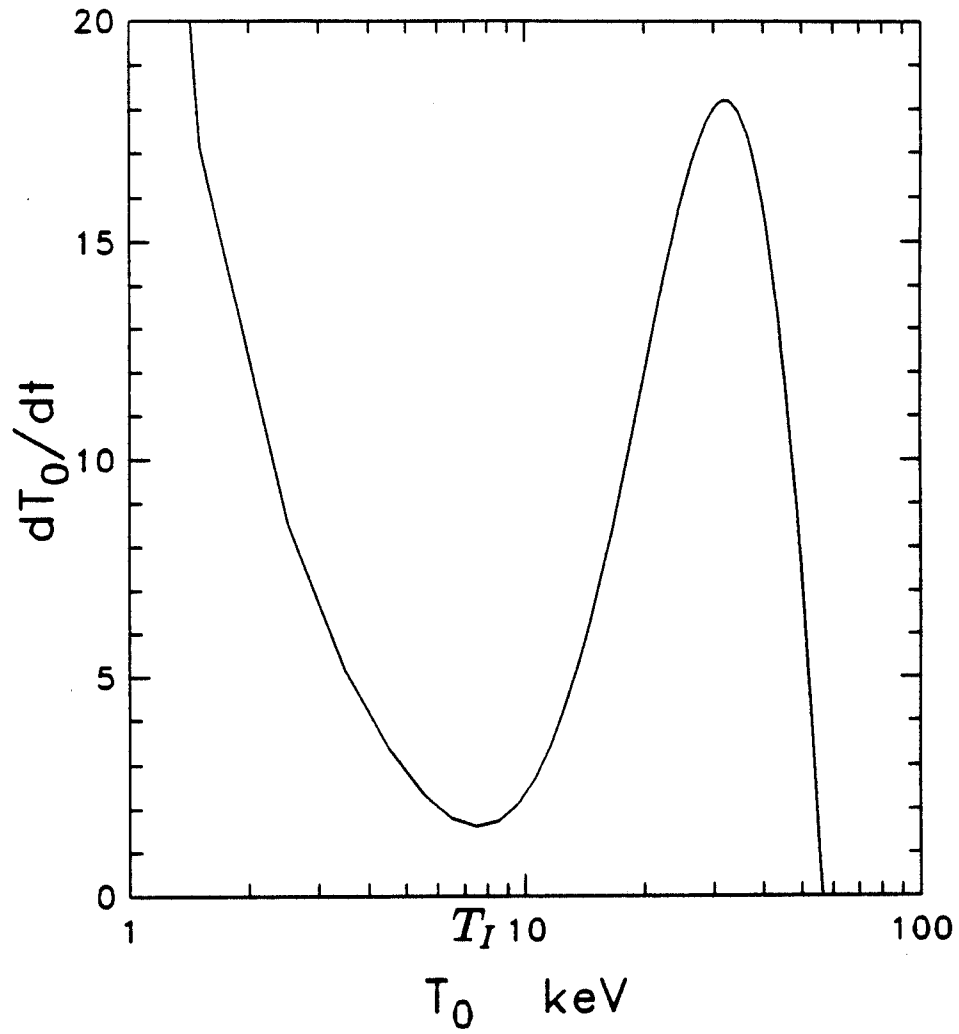


Figure 2: \dot{T} vs T plot illustrating the case of ohmic ignition

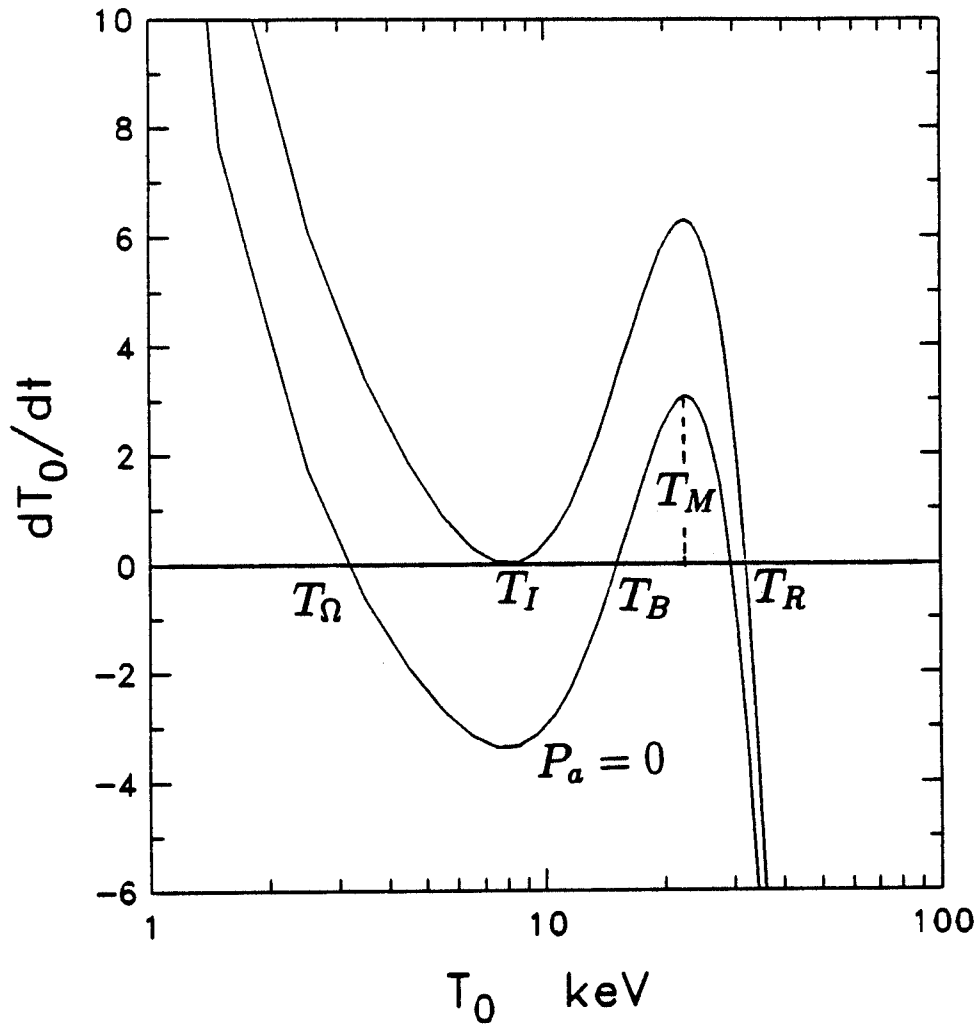


Figure 3: \dot{T} vs T plot illustrating the case of auxiliary power ignition

and corresponds to pure ohmic ignition since $P_a = 0$; see Fig. 2. Note that when T exceeds T_I the plasma temperature will runaway.

The second method to achieve $\dot{T} > 0$ applies when economic and/or technological considerations prevent the design of an ohmically ignited machine. In this case the minimum of the \dot{T} curve can be made positive if sufficient auxiliary power is supplied to the plasma. This type of ignition is denoted as ignition with auxiliary power; see Fig. 3. Once T_I is exceeded, the auxiliary power can be gradually decreased shifting operation to $T = T_B$ on the $P_a = 0$ curve. Note that at $T = T_B$ the system is susceptible to a thermal runaway since $\dot{T}(T_B) > 0$. This is the problem of burn control.

For non-ohmically ignited systems the form of the \dot{T} vs T curve in Fig. 3 is the most desirable because, with the aid of auxiliary power, access is provided to the thermal equilibrium point T_B along the $P_a = 0$ curve.

A second, and not as desirable, situation is illustrated in Fig. 4. Again, with sufficient auxiliary power, the minimum of the \dot{T} curve can be made positive. However, the corresponding curve for $P_a = 0$ has a maximum which is below the axis. Thus, once T exceeds T_I , the auxiliary power cannot be completely shut off since no thermal equilibrium point exists. Instead, the power is reduced as much as possible until the maximum of \dot{T} is just tangent to the axis. Since P_a is now not equal to zero at the steady state equilibrium temperature T_B , the system acts as an amplifier with gain $Q = P_n/P_a$ where P_n is the fusion neutron power.

The third situation to consider is illustrated in Fig. 5. Here, the confinement is so poor that \dot{T} vs T is a monotonically decreasing function for any auxiliary power. There is no potential region for alpha dominated operation and only the ohmic equilibrium temperature T_Ω is possible. This corresponds to "no fusion" and is obviously the least desirable regime of operation.

The natural definition of ignition thus requires a region of thermal runaway in the \dot{T} vs T diagram regardless of how small. The precise mathematical definitions [4] of the regimes of interest can be conveniently summarized as follows

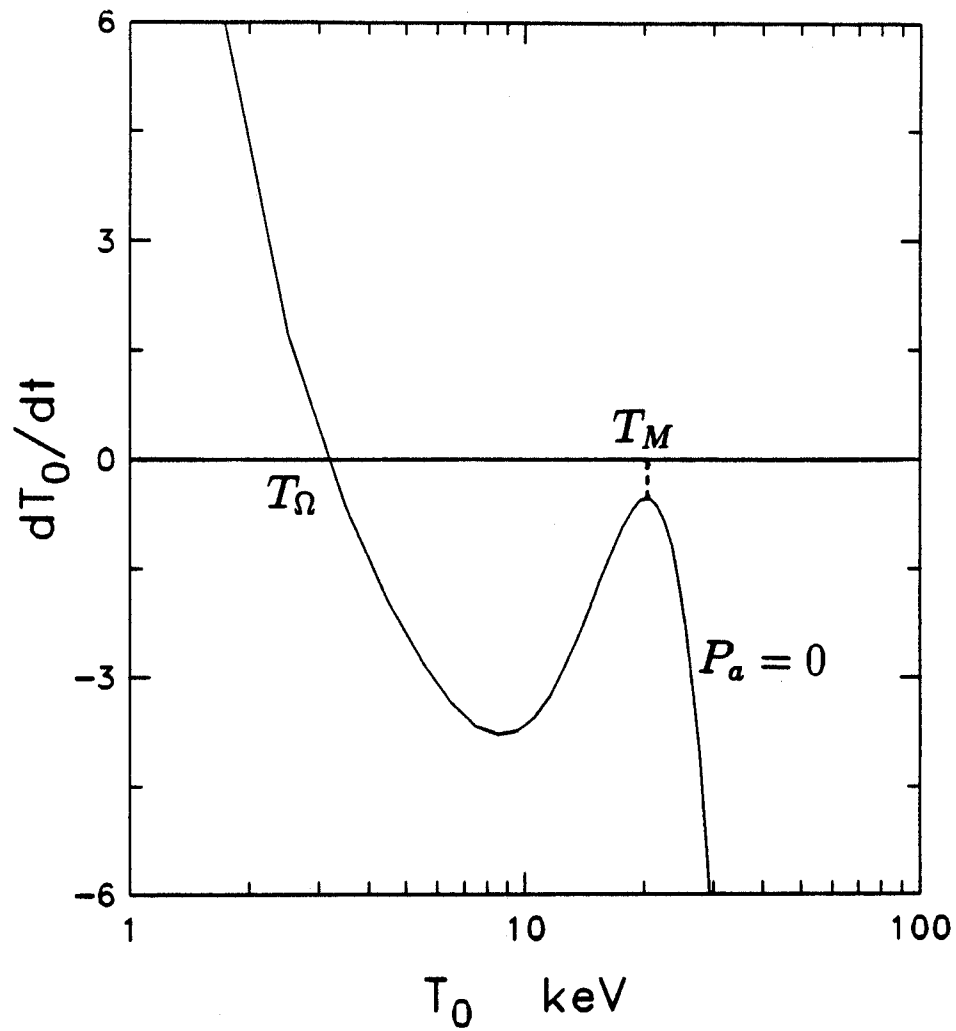


Figure 4: \dot{T} vs T plot illustrating the case of auxiliary power ignition in a low performance machine

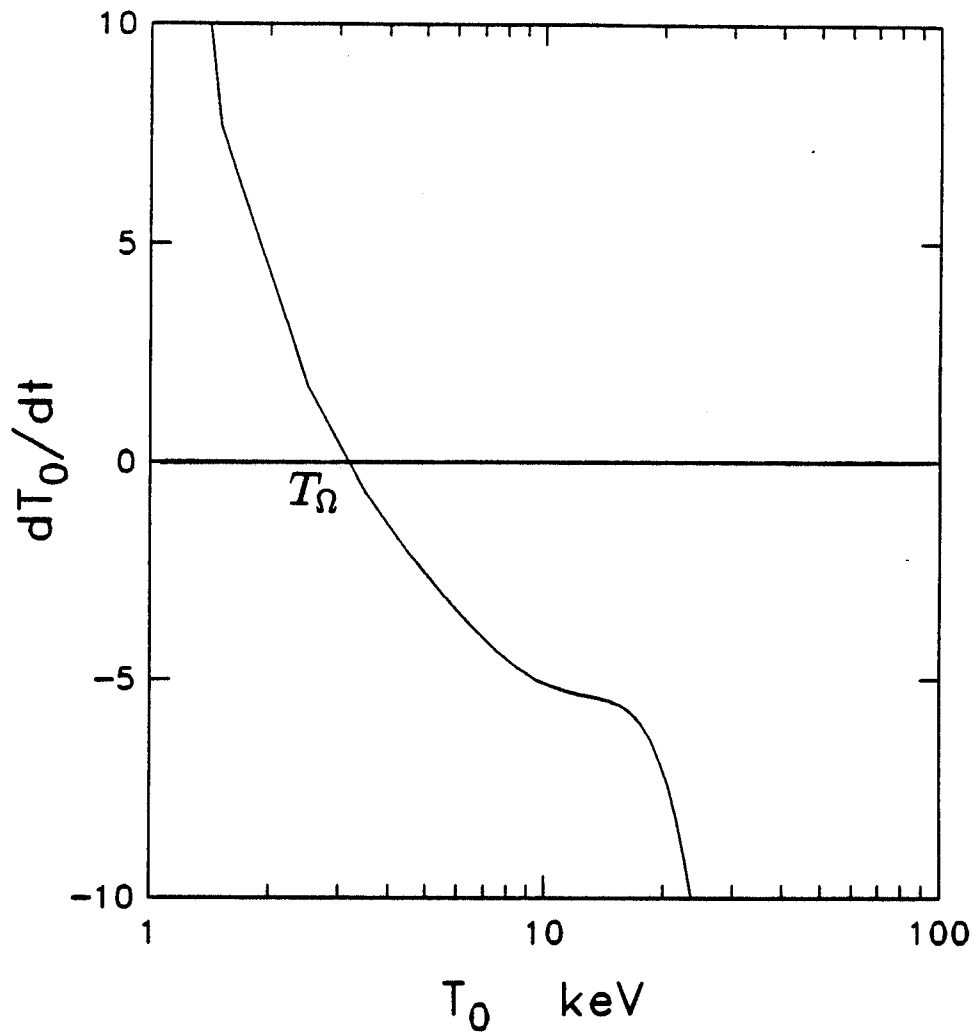


Figure 5: \dot{T} vs T plot illustrating the case of nonignited operation

1. Pure Ohmic Ignition

$$\dot{T}(T_I, W, N, \Pi = 0) = 0 \quad (10)$$

$$\frac{\partial \dot{T}}{\partial T}(T_I, W, N, \Pi = 0) = 0 \quad (11)$$

2. Auxiliary Power Aided Ignition

$$\dot{T}(T_I, W, N, \Pi) = 0 \quad (12)$$

$$\frac{\partial \dot{T}}{\partial T}(T_I, W, N, \Pi) = 0 \quad (13)$$

$$\dot{T}(T_M, \Pi = 0) > 0 \quad (14)$$

The significance of the temperature T_M can be inferred by examining Fig. 3.

3. Auxiliary Power Aided Amplification

$$\dot{T}(T_I, W, N, \Pi) = 0 \quad (15)$$

$$\frac{\partial \dot{T}}{\partial T}(T_I, W, N, \Pi) = 0 \quad (16)$$

$$\dot{T}(T_M, \Pi = 0) < 0 \quad (17)$$

4. No Fusion

$$\frac{\partial \dot{T}}{\partial T}(T_I, W, N, \Pi) < 0 \quad (18)$$

The ignition characteristics can also be observed by examining the contours of constant auxiliary power. These contours usually referred to as Plasma Operating Contours (POPCON) [5] are obtained by calculating the auxiliary power required to make $dT/dt = 0$ at a combination of plasma

density and temperatures. Thus a POPCON represents steady state behavior. A typical POPCON is shown in Fig. 6. The ignition temperature T_I , satisfying Eqs. (10, 11) form the contour indicated by the dots in Fig. 6. This contour goes through the “Cordey pass” – the point at which both $\dot{T} = 0$ and $d\dot{T}/dT = 0$ are satisfied with the least amount of auxiliary power. This contour which is henceforth called Marginal Ignition Ridge (MIR) is important since it is the boundary between the regions of negative and positive growth rates for the plasma temperature.[6]

In the following section the ignition requirements for systems falling in regimes 1 and 2 are investigated, and the boundaries separating these regions in the parameter space of auxiliary power *vs* performance are presented.

2.1 Ohmic Ignition

An ohmically ignited plasma is one that gains access to the alpha dominated regime solely by means of ohmic heating; no auxiliary power is required (i.e., $\Pi = 0$). This is highly desirable in view of the scientific and technological complexities associated with auxiliary power. The major difficulty with ohmic ignition is that it requires large values of W which ultimately translates into high cost.

The minimum value of W required for ohmic ignition is determined by the condition that the \dot{T} vs T curve becomes tangent to the T axis at $T = T_I$. See Fig. 3. This is expressed by Eqs. (10, 11). Solving these equations gives the minimum $W = W(N)$. The function $W(N)$ itself has a well defined minimum with respect to N as it is shown in Fig. 7. Setting $dW/dN = 0$ then gives the absolute minimum W and corresponding N and T for ohmic ignition. These values are given in Table 1 for the generic scalings, the ohmic scaling, and the auxiliary scaling. Also given are the values for $n\tau_E$.

By writing the function \mathcal{F} in the general form

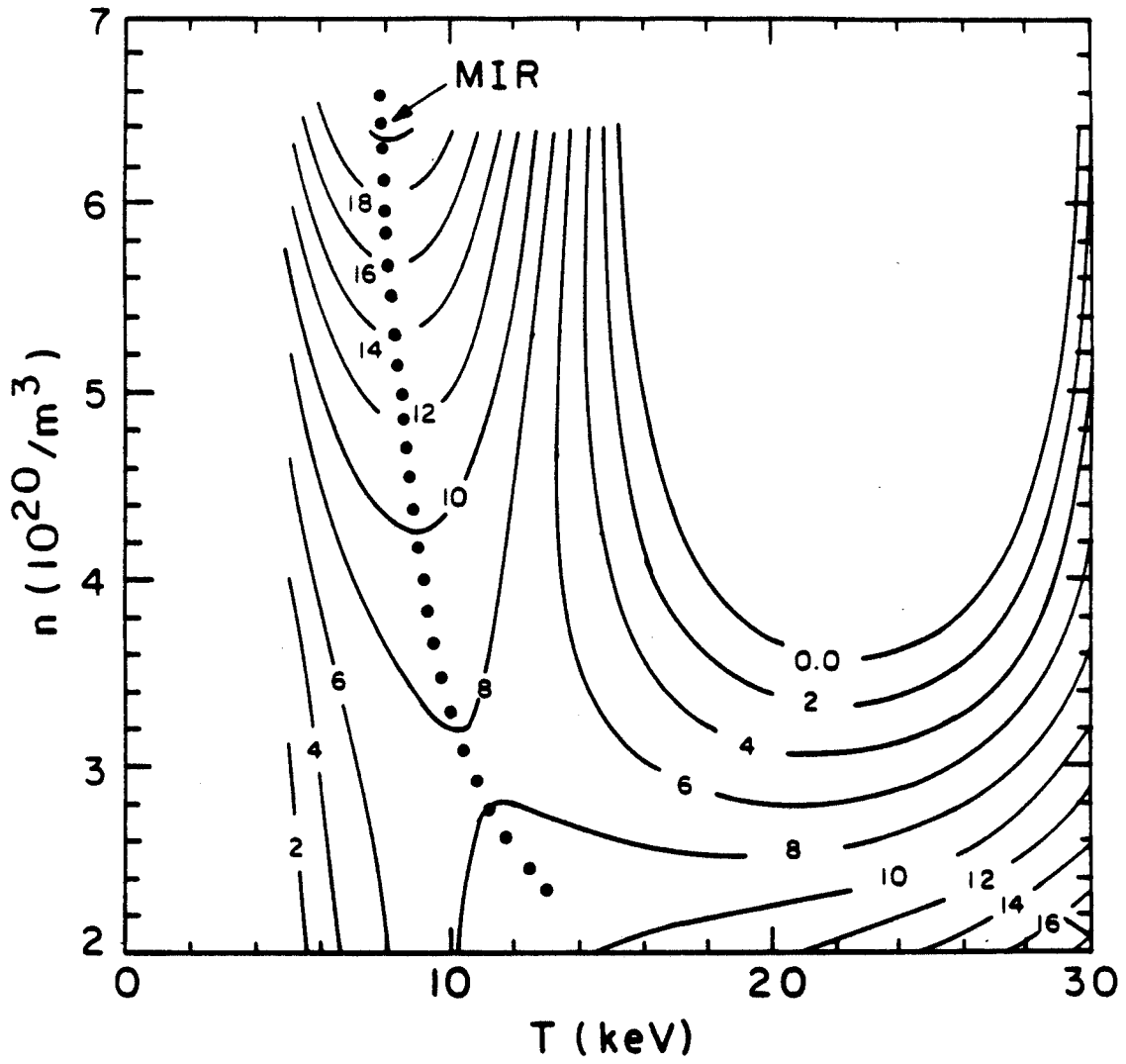


Figure 6: Typical POPCON plot indicating the Marginal Ignition Ridge (MIR)

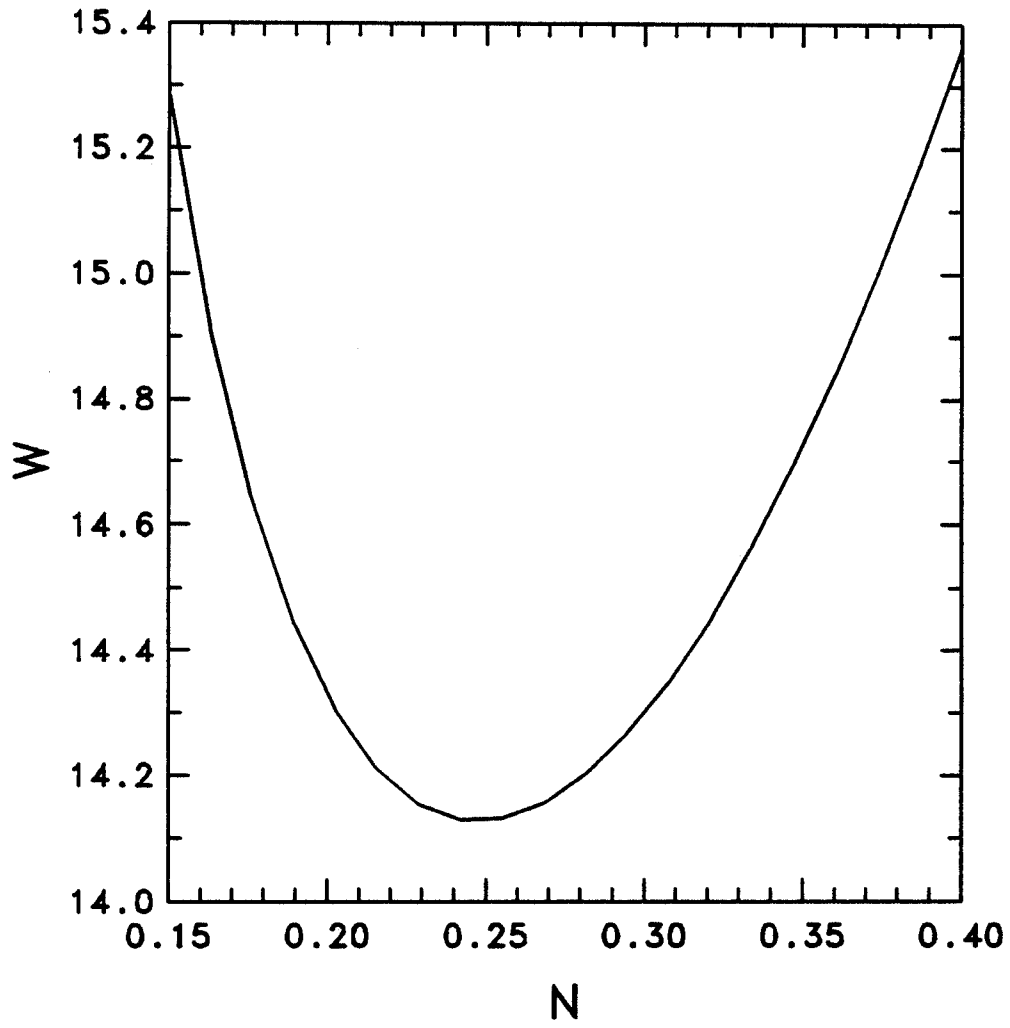


Figure 7: A plot of the performance parameter W as a function of the Murakami density factor N

Table 1: Critical Parameters for Ohmic Ignition

	Generic	Ohmic	Auxiliary1	Auxiliary2
W	14.2	19.5	14.6	22.92
T_I	11.39	7.06	9.89	7.07
N	0.249	0.576	0.371	0.679
$n\tau_E$	3.51	11.20	5.42	15.56

$$\mathcal{F} = \frac{N^\alpha}{T^\beta} \quad (19)$$

the complete parameter range of possible N and T dependances can be investigated. By taking $\alpha = 0$ the minimum values of W and the corresponding N are plotted in Fig. 8 as a function of the exponent β . Note that the variation of W with β is very small. Also note that the values for N are well below the Murakami limit for all β . Interestingly, as seen from Fig. 8, and from table 1 the minimum W shows very little variation whereas $n\tau_E$ varies by more than a factor of three. Even so, a value of $W \sim 15$ is sufficiently large that the resulting machine cost would exceed the economic resources allocated for currently envisaged next generation ignition experiments.

2.2 Auxiliary Power Ignition

When W is less than the value required for ohmic ignition, sufficient auxiliary power guarantees access to α dominated operation as long as $\dot{T}(T_M) > 0$ on the $P_a = 0$ curve (see Fig 3 for an indication of the temperature T_M). The condition that the \dot{T} curve be tangent to the T axis at T_M defines the minimum value of W required for auxiliary power ignition.

The solution of Eqs. (12, 13) gives the minimum $W = W(N)$. In this regime W monotonically decreases as N increases. Thus, the absolute minimum value of W occurs when N reaches the Murakami limit. Table 2 gives

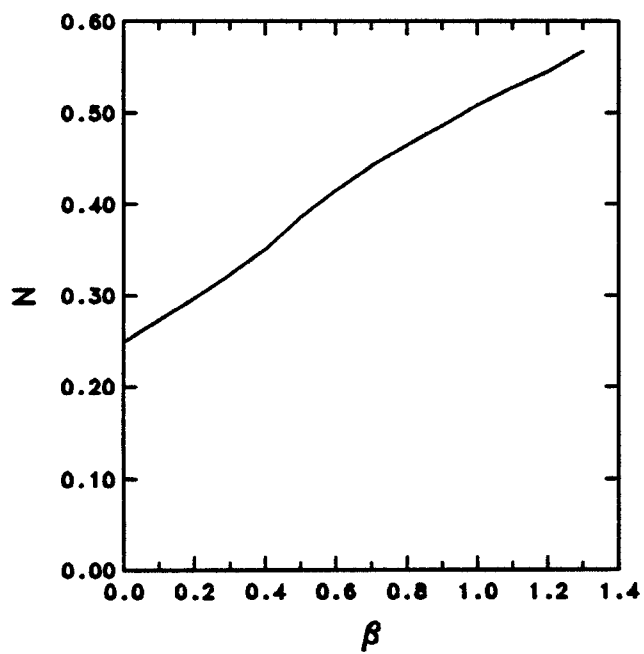
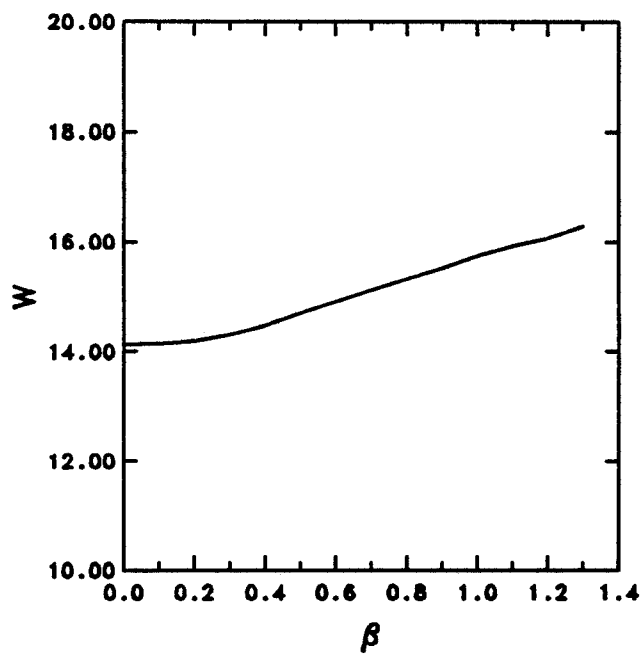


Figure 8: A plot of the optimum values for W and N as a function of the exponent β in Eq. (19)

Table 2: Critical Parameters for Auxiliary Power Ignition

	Generic	Ohmic	Auxiliary1	Auxiliary2
W	1.63	1.63	1.75	2.14
T_I	34.2	34.2	25.1	19.13
N	1.4	1.4	1.4	1.4
$n\tau_E$	2.28	2.28	2.45	2.99

the values of W , T_a , N and $n\tau_E$ for the generic scaling, the ohmic scaling and the auxiliary scalings.

Observe that the value of W is much smaller than that required for ohmic ignition.

2.3 Non-Ignited Operation

If W is less than the value given in Table 2, the \dot{T} vs T diagram for $P_a = 0$ assumes the form illustrated in Fig. 5. In this case there is only one steady state operating point corresponding to an ohmically heated discharge, $T = T_\Omega$. There is no steady state operation dominated by alpha power heating. Consequently, this regime is non-ignited and is discussed no further.

3 The Minimum Auxiliary Power for Ignition

Another topic of interest concerns the minimum auxiliary power required for ignition. It is important to minimize this power for two reasons. First, since auxiliary power is technologically complicated and economically expensive, it is desirable to keep the requirements as low as possible. Second, and more critical, is the experimental evidence that the empirical scaling relations are more reliable and optimistic in the ohmic dominated regime. Hence, minimizing P_a also minimizes the uncertainties associated with τ_E

in the auxiliary heated regime. In this connection it is more appropriate to minimize P_a/P_Ω rather than P_a itself. Here P_Ω is the total ohmic power.

In order to calculate $(P_a/P_\Omega)_{min}$, the value of W is fixed at some intermediate value between the ohmic ignition and auxiliary power ignition boundaries. The ignition condition is given by

$$\dot{T}(T, W, N, \Pi) = 0 \quad (20)$$

$$\frac{\partial \dot{T}}{\partial T}(T, W, N, \Pi) = 0 \quad (21)$$

Solving these equations gives $\Pi = \Pi(N, W)$. This is substituted into the following

$$\Gamma \equiv \frac{P_a}{P_\Omega} = \frac{C_a}{C_\Omega} \Pi T^{3/2} \quad (22)$$

yielding $\Gamma = \Gamma(N, W)$. For higher values of W , Γ has a minimum with respect to N (see Fig 7) that is less than the Murakami limit. At smaller W , the minimizing N exceeds the Murakami limit. In this situation the minimum W is obtained by setting $N = 1.4$, the Murakami limit.[3]

Fig. 9 shows the variation of $(P_a/P_\Omega)_{min}$ with W . As expected P_a/P_Ω is a decreasing function of W , illustrating the basic tradeoff between physics reliability and cost. Observe that P_a/P_Ω is a very steep function of W for small W . Thus, for $W < 5$ the plasma is operating in a particularly sensitive region of parameter space. Also there is relatively small variation in P_a/P_Ω for the different scaling relations.

4 Coupling Physics and Engineering

Up to this point the goal was to estimate the values of the various physics based parameters W, N, Π . These parameters are directly related to the physics considerations as represented by the 0-D model. In this section the ignition ideas developed in the previous sections are coupled to fundamental engineering considerations of both the toroidal and the ohmic heating coils resulting in optimized tokamak designs.

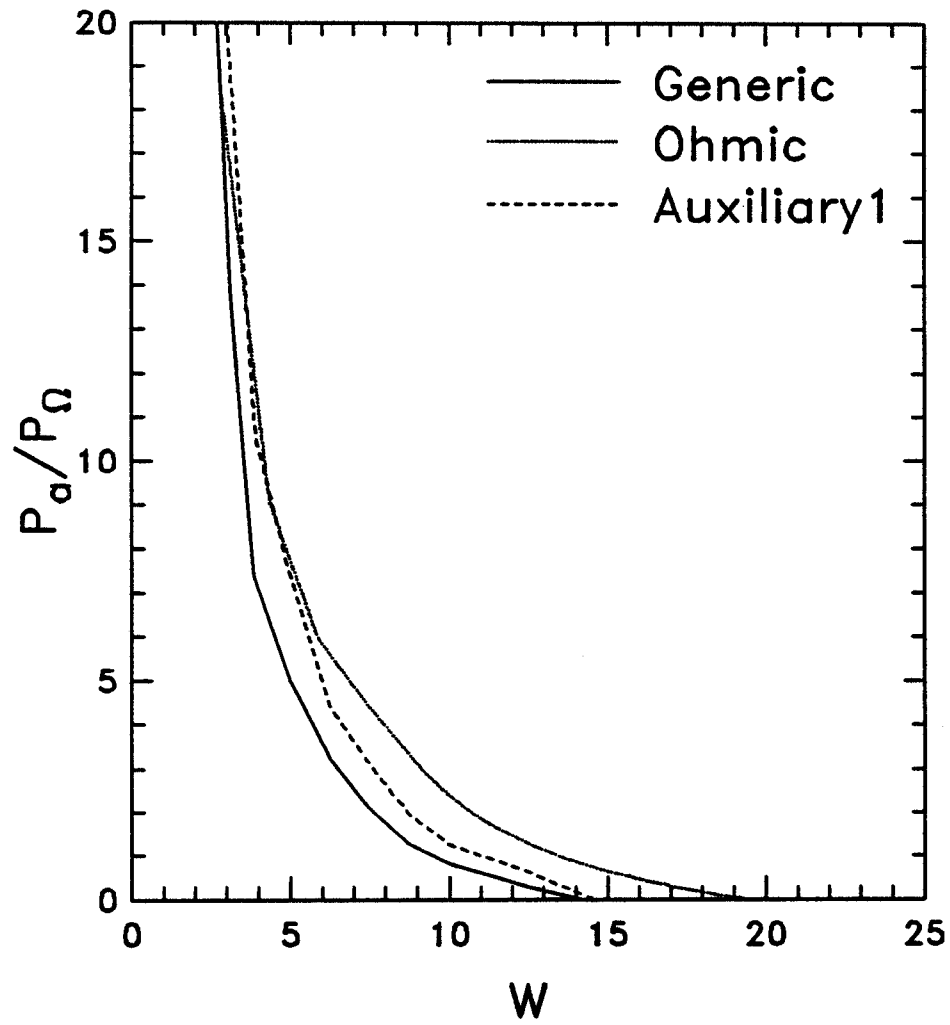


Figure 9: A plot of the optimum value of P_a/P_Ω as a function of the parameter W

4.1 Optimized Ignition Physics and Machine Performance

The first step is to develop a sharply defined goal of “optimized ignition”. There are two main issues to consider. First, since we have been driven to auxiliary power aided ignition because of the prohibitive economic limitations imposed by pure ohmic ignition, the total machine cost is clearly one of the most important problems. Second, and somewhat less quantitative, is the relatively high physics uncertainty associated with auxiliary power confinement scaling as compared to the ohmic scaling.

Consider now in more detail, the questions of cost and physics uncertainty. Optimizations based purely on cost tend to place too much emphasis on auxiliary power. Large values of P_a relative to P_Ω are required, resulting in operation in a regime of high physics uncertainty. Thus, while the cost is minimized, the probability of success is not.

In this analysis a different approach is adopted. It is assumed that virtually all of the available economic resources are dedicated to the basic machine (excluding auxiliary power). The machine design is then optimized by minimizing the auxiliary power required for ignition. This philosophy places a high weight on minimizing the physics uncertainty, and as it is shown below it does not add significantly to the economic constraints as relatively small values of P_a are required.

It can be argued that the tokamak performance is approximately proportional to the cost of the TF system. Furthermore, the overall TF design is strongly driven by the coil throat, the most critical element in the magnet. By assuming that the cost of coil throat is proportional to its volume V , V can be adopted as a universal measure of machine performance. It is then possible to relate the geometric quantity \widehat{W} to the coil throat volume V . In this way \widehat{W} is eliminated in terms of the volume V

Minimizing the physics uncertainty actually implies minimizing P_a with respect to a given ohmic power P_Ω . A minimization of the absolute value of

P_a leads to the unphysical limit $B_0 \rightarrow \infty$, $a \rightarrow 0$. Since $a \rightarrow 0$, the plasma volume approaches zero implying that no auxiliary power is required. Even so, in this limit, the ratio P_a/P_Ω can be large implying high physics uncertainty.

Thus, in the analysis that follows, the quantity P_a/P_Ω required for ignition is minimized, subject to the constraint of a fixed volume V set at the maximum value permissible by economic constraints. When the calculation is complete it is shown a posteriori that the auxiliary power cost is not prohibitive and that the equilibrium burn temperature is indeed in the ignited regime of operation.

The optimization procedure can be summarized mathematically as follows. The quantity P_a/P_Ω is easily found from Eq. (1).

$$\frac{P_a}{P_\Omega} = \frac{C_a}{C_\Omega} \Pi T^{3/2} \equiv U(T, \Pi, N, W, q_*, \kappa, a, R_0) \quad (23)$$

U is to be minimized subject to the condition that the plasma is ignited.

$$\dot{T}(T_I, \Pi_I, N, W, q_*, \kappa) = 0 \quad (24)$$

$$\frac{\partial \dot{T}}{\partial T}(T_I, \Pi_I, N, W, q_*, \kappa) = 0 \quad (25)$$

and the constraint that the TF coil throat volume V is fixed. In the next section it is shown that $V = V(\widehat{W}, a, R_0, \kappa, q_*)$ so that the fixed volume constraint becomes

$$V(\widehat{W}, a, R_0, \kappa, q_*) = \text{const.} \quad (26)$$

In principle, Eqs. (24) and (25) are solved for T_I and Π_I , and Eq. (26) for \widehat{W} . These results are substituted into Eq. (23) yielding

$$U = U(N, q_*, \kappa, a, R_0; V) \quad (27)$$

The quantity U is then minimized with respect to N, q_*, κ, a, R_0 holding V fixed. In practice, the dependence of U on q_* and κ is monotonic implying that these quantities must be set to their extremum values as determined by physics: $q_* = 2, \kappa = 2$. What remains is a three dimensional minimization of U with respect to N, a, R_0 .

4.2 TF Coil Design

The one remaining relation required is that expressing the throat volume, V , in terms of the ignition parameters. The coil model described below is sufficient for this purpose. The critical assumption is that V is determined by stress considerations on the inner leg of the magnet.

The coil model is deliberately simplified for purposes of pedagogical clarity and to avoid any false impressions of unjustified accuracy. It is important to realize that the goal of this work is to demonstrate trends rather than to arrive at a precise final design. Thus, while the results are only semi-quantitatively correct in detail, they quite accurately describe the features and directions of the optimized design.

Consider the rectangular coil model illustrated in Fig. 10. The distances b_1, b_2 and b_3 separate the plasma from the TF magnet and provide space for the first wall, divertor, RF antennae, etc. The values of b_1 and b_2 are taken from the current CIT design and are assumed to be known quantities. The value of b_3 is scaled with the minor radius according to the relation.[7]

$$b_3 = 0.88 a + 0.5 \quad (28)$$

The thickness of the coil throat is denoted by c , and it is this quantity that is crucial in determining the volume V . The value of c is found by calculating the Tresca stress on the inner leg of the magnet and setting it equal to its maximum allowable value $\sigma_m \approx 500 \text{ MPa}$.

The analysis begins with the evaluation of V . A short calculation gives

$$V = 4\pi c(\kappa a + b_3)(R_0 - a - b_1 - c/2) \quad (29)$$

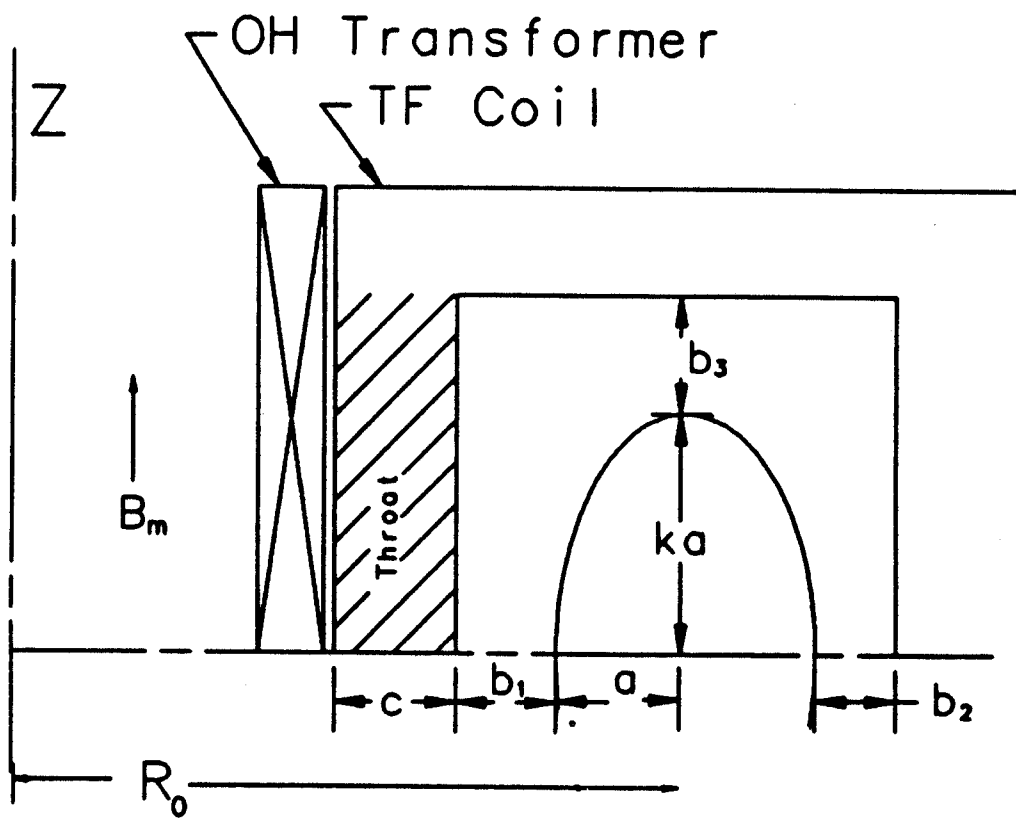


Figure 10: A toroidal coil model

In order to obtain a reference case, for comparing the accuracy of the model, the CIT parameters are considered (i.e. $R_0 = 2.1 \text{ m}$, $a = .64 \text{ m}$, $\kappa = 2.0$, $b_1 = .17 \text{ m}$, $b_2 = .6 \text{ m}$, $b_3 = .86 \text{ m}$, $c = .43 \text{ m}$, $B_0 = 11 \text{ T}$, $I = 11 \text{ MA}$, $\sigma_m = 500 \text{ MPa}$). This gives a throat volume $V = 12.4 \text{ m}^3$ for the reference case.

Next, consider the vertical hoop stress. The total vertical force F_Z acting on the upper half of the magnet can be approximated by

$$F_Z \approx \frac{2\pi}{\mu_0} B_0^2 R_0 (a + \bar{b}) \quad (30)$$

where

$$\bar{b} = \frac{b_1 + b_2}{2} \quad (31)$$

This force is assumed to be distributed equally between the inner and outer magnet legs. It produces a tensile stress σ_t that is much larger on the inner leg because the stress area of the inner leg, $A_Z = \pi(R_2^2 - R_1^2)$, is much smaller. A simple calculation gives

$$\sigma_t = \frac{F_Z}{2A_Z} = \frac{B_0^2}{2\mu_0} \frac{R_0 (a + \bar{b})}{c(R_0 - a - b_1 - c/2)} \quad (32)$$

The second stress to be considered is due to wedging. As a simple approximation, it is useful to calculate the relation between the wedging force and the hoop force in the thin coil limit $c \rightarrow 0$. Using this relation, it is then straightforward to estimate the Tresca stress, using the finite thickness tensile stress [Eq. (32)].

In the thin coil limit the net centering force is approximately given by

$$F_R \simeq -\frac{2\pi}{\mu_0} B_0^2 R_0^2 (\kappa a + b_3) \left[\frac{1}{R_0 - a - b_1} - \frac{1}{R_0 + a + b_2} \right] \quad (33)$$

The centering force F_R produces a wedging stress

$$\sigma_w = \frac{F_R}{2\pi A_R} \quad (34)$$

where $A_R \approx 2(\kappa a + b_3)c$. Substituting Eq. (33) into Eq. (34) gives

$$\sigma_w \approx -\frac{B_0^2 R_0^2}{2\mu_0 c} \left[\frac{1}{R_0 - a - b_1} - \frac{1}{R_0 + a + b_2} \right] \quad (35)$$

In the thin coil limit, a comparison of Eqs. (32) and (35) indicates that

$$\left. \frac{\sigma_w}{\sigma_t} \right|_{c \rightarrow 0} = -\frac{2}{1 + \epsilon_2} \quad (36)$$

Where ϵ_2 is given by

$$\epsilon_2 = \frac{a + b_2}{R_0} \quad (37)$$

Now assume for simplicity that Eq. (36) is valid for finite thickness coils as well. Under this assumption, the Tresca stress $\sigma_T \equiv \sigma_t - \sigma_w$ can be written as

$$\sigma_T = \frac{B_0^2}{2\mu_0} \left(\frac{3 + \epsilon_2}{1 + \epsilon_2} \right) \frac{(a + \bar{b}) R_0}{c(R_0 - a - b_1 - c/2)} \quad (38)$$

By setting $\sigma_T = \sigma_m$ (the maximum allowable stress) in Eq. (38) the coil thickness is given by

$$c = \frac{B_0^2}{2\mu_0 \sigma_m} \left(\frac{3 + \epsilon_2}{1 + \epsilon_2} \right) \frac{(a + \bar{b}) R_0}{c(R_0 - a - b_1 - c/2)} \quad (39)$$

By substituting Eq. (39) into Eq. (29) the coil volume is given by

$$V = \frac{\pi B^2 R_0}{\mu_0 \sigma_m} \left\{ \left[\frac{1}{(2a + b_1 + b_2)(\kappa a + b_3)} \right] \left[\frac{R_0 + a + b_2}{(3R_0 + a + b_2)} \right] \right\}^{-1} \quad (40)$$

Equation (40) is the desired relation. It is the equation that couples the ignition physics and the engineering. Since the parameter \widehat{W} depends on the plasma geometry the coil volume given by Eq. (40) can alternatively be expressed as a function of \widehat{W} . In order to check the calibration of this model the CIT parameters are used. By solving Eq. (40) for B and substituting the CIT parameters gives $B = 10.7$ Tesla which is in good agreement with the 11 Tesla CIT design.

In practice there are several important limits which prevent small R_0 . Certainly, the geometric condition $R_0 > a + b_1 + c$ must be satisfied. An even stronger limit on R_0 results from the volt-second requirements of the ohmic transformer, and it is investigated next.

4.3 OH Coil Design: Volt Second Requirements.

In this section a derivation of the minimum major radius that satisfies the volt-second requirements of the ohmic transformer is presented.

4.3.1 Basic Constraint

The basic constraint defining the volt-second requirements can be written as

$$\Delta\psi = kLI \quad (41)$$

Here, $\Delta\psi$ is the flux swing in the transformer, I is the plasma current, and L is the plasma inductance, which can be approximated as [8]

$$L = \mu_0 R_0 \left[\ln \left(\frac{8R_0}{a\kappa^{1/2}} \right) - \frac{7}{4} \right] \quad (42)$$

The parameter k is a constant and typically $k \approx 1.2$. This guarantees sufficient volt-seconds to bring the current from zero to its final value as well as maintaining the plasma for an extended period of flat top operation.

In equation (41) it is also convenient to express I in terms of B_0 and q_*

$$I = \frac{2\pi a^2 \kappa B_0}{\mu_0 R_0 q_*} \quad (43)$$

4.3.2 Evaluation of $\Delta\psi$

In order to evaluate $\Delta\psi$ it is assumed that the magnetic field in the transformer is double swung from $-B_m$ to $+B_m$. For a double swing system

$$\Delta\psi = 2(\psi_1 + \psi_2) \quad (44)$$

where ψ_1 is the flux in the vacuum region and ψ_2 is the flux in the coil. The final value of the flux in the vacuum region is

$$\psi_1 = \pi R_a^2 B_m \quad (45)$$

where the transformer geometry is illustrated in Fig. 11. The flux in the coil itself is easily found by noting that for a uniform current density

$$B = B_m \left(\frac{R_b - R}{R_b - R_a} \right) \quad R_a < R < R_b \quad (46)$$

A simple calculation then gives

$$\psi_2 = \frac{\pi B_m}{3} (R_b - R_a) (R_b + 2R_a) \quad (47)$$

Therefore $\Delta\psi$ becomes

$$\Delta\psi = 2\pi B_m \left[R_a^2 + \frac{1}{3} (R_b - R_a) (R_b + 2R_a) \right] \quad (48)$$

4.3.3 Relate the maximum field B_m to the maximum stress σ_p

Typically $\sigma_p \approx 330 \text{ MPa}$ for CIT. The local Tresca stress in a straight solenoid has the form[9]

$$\sigma_T(R) = \frac{B_m^2}{\mu_0} \left(\frac{R_a^2}{R_b^2 - R_a^2} \right) \left(\frac{R_b^2}{R^2} \right) \quad (49)$$

Unlike the TF coil, σ_T is a strong function of R in the ohmic transformer coil, particularly if the coil is thick.

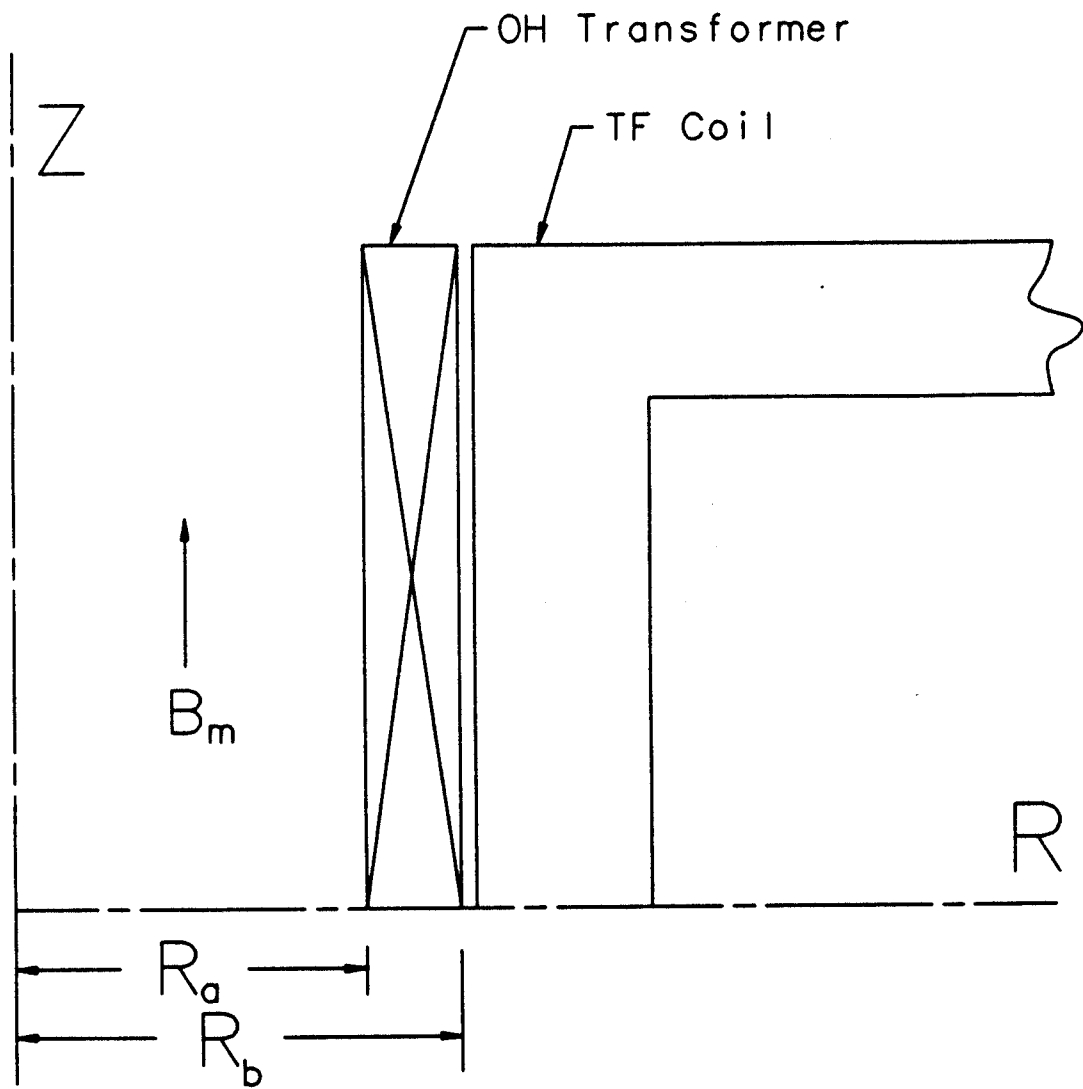


Figure 11: The ohmic heating coil model

In general, it is required that the peak to average stress ratio in the OH system be less than some value η . For CIT $\eta \simeq 1.5$. This serves to determine the ratio R_b/R_a . The peak stress occurs at $R = R_a$ and is given by

$$\sigma_T(R_a) = \frac{B_m^2}{\mu_0} \left(\frac{R_b^2}{R_b^2 - R_a^2} \right) \quad (50)$$

The average stress is defined as $\overline{\sigma_T} \equiv \int \sigma_T dR / \int dR$, and is given by

$$\overline{\sigma_T} = \frac{B_m^2}{\mu_0} \left(\frac{R_b R_a}{R_b^2 - R_a^2} \right) \quad (51)$$

Computing the ratio $(\sigma_T(R_a) / \overline{\sigma_T}) = \eta$ leads to

$$\frac{R_b}{R_a} = \eta \quad (52)$$

4.3.4 Intermediate form of the Volt-Seconds constraint

Combining the results just derived, setting $\overline{\sigma_T} = \sigma_p$, and noting that $R_b = R_0 - a - b_1 - c$, the following form for the volt-seconds constraint is obtained.

$$\begin{aligned} & k \left(\frac{\kappa a^2 B_0}{q_*} \right) \left(\ln \frac{8R_0}{a\kappa^{1/2}} - \frac{7}{4} \right) \\ & = (\mu_0 \sigma_p)^{1/2} \left(\frac{\eta^2 - 1}{\eta} \right)^{1/2} \left[\frac{\eta^2 + \eta + 1}{3\eta^2} \right] (R_0 - a - b_1 - c)^2 \quad (53) \end{aligned}$$

Substituting the values $\sigma_p = 330 \text{ MPa}$, $\eta = 1.5$, $k = 1.2$ leads to

$$R_0 = a + b_1 + c + .4 \left(\frac{\kappa B a^2}{q_*} \right)^{1/2} \quad (54)$$

4.3.5 Final form of the Volt-Seconds constraint

The final step in the calculation is the elimination of the coil thickness c from Eq. (54). The quantity c is expressed in terms of V from Eq. (29), the defining relation for the coil throat volume. Equation (29) can be written as

$$c^2 - 2(R_0 - a - b_1)c + \frac{V}{2\pi(\kappa a + b_3)} = 0 \quad (55)$$

Solving for c yields

$$c = R_0 - a - b_1 - \left[(R_0 - a - b_1)^2 - \frac{V}{2\pi(\kappa a + b_3)} \right]^{1/2} \quad (56)$$

Substituting into Eq. (54) leads to the following expression for R_0

$$R_0 = a + b_1 + 0.4 \left(\frac{\kappa a^2 B}{q_*} + \frac{V}{\kappa a + b_3} \right)^{1/2} \quad (57)$$

Equation (57) is the desired relation, giving $R_0 = R_0(B, a, V, \kappa, q_*)$.

Substituting the calibration values on the right hand side gives $R_0 = 2.1$, again indicating an accurate calibration between the simple model and the CIT design used for calibration. Thus, in the full optimization the geometric factor \widehat{W} is expressed as a function of V by Eq. (40) with R_0 evaluated from Eq. (57).

5 Results

The physics and the engineering are coupled through Eqs. (24, 25, 40, 57). Eqs. (24 and 25) represent the ignition condition, and Eqs. (40, 57) characterize the toroidal field and ohmic heating coils. The optimized designs are obtained by simultaneously solving Eqs. (24, 25, 40, 57) and by minimizing the quantity

Table 3: The Parameters α_j corresponding to Eq. (59) for various confinement scalings

	α_1	α_2	α_3	α_4	α_5
Goldston	0.75	-0.37	1.0	1.0	0.5
Neo-Alcator	0.0	1.0	2.0	0.0	0.5
Kaye-Goldston	0.13	-0.49	1.17	1.24	0.28
ITER	0.1	0.3	1.3	0.85	0.5

$$\frac{P_a}{P_\Omega} = U(N, a, T_I, \Pi_I, W, R_0) \quad (58)$$

Note that the kink safety factor q_* and the ellipticity κ do not appear in the above equation. Specifically q_* and κ are considered constant and in the following results they have the values $q_* = 2.0$ and $\kappa = 2.0$. The four parameters T_I , Π_I , W , R_0 are determined from Eqs. (24, 25, 40, 54). In turn the quantity P_a/P_Ω is minimized in the N, a space.

The first step in the solution procedure is the characterization of the parameter \widehat{W} . In general the parameter \widehat{W} can be written as

$$\widehat{W} = C_1 R_0^{\alpha_1} a^{\alpha_2} B^{\alpha_3} I^{\alpha_4} \kappa^{\alpha_5} \quad (59)$$

By adjusting the parameters α_j various confinement scalings can be simulated. Table 3 gives the values of the parameters $\alpha_1, \alpha_2, \alpha_3, \alpha_4, \alpha_5$ for Neo-Alcator, Goldston, Kaye Goldston, and ITER P-89[10] confinement scalings. The form for the auxiliary power dependence is not included in \widehat{W} . It is incorporated in the function \mathcal{F} (see Eq. 7).

Another parameter that must be given is the coil throat volume V . The coil volume is a constraint in the calculation and the optimization is performed subject to a fixed coil volume. The results that follow correspond to $V = 25m^3$ which represents the throat volume of the present CIT design.

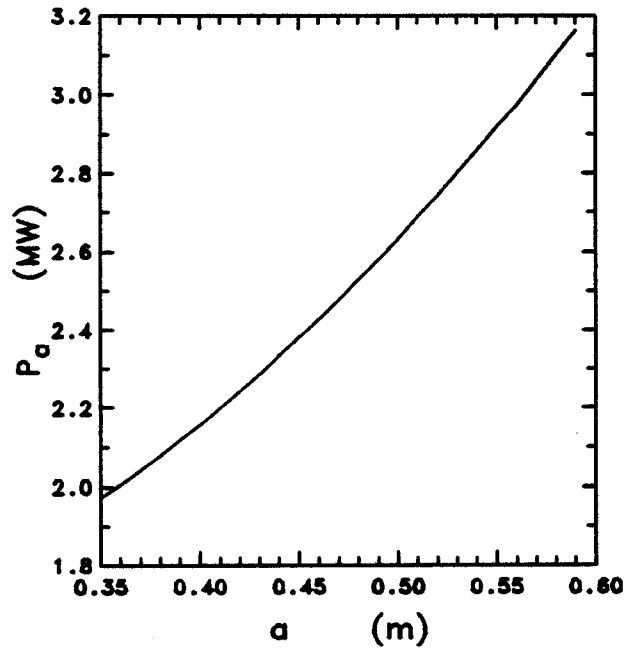
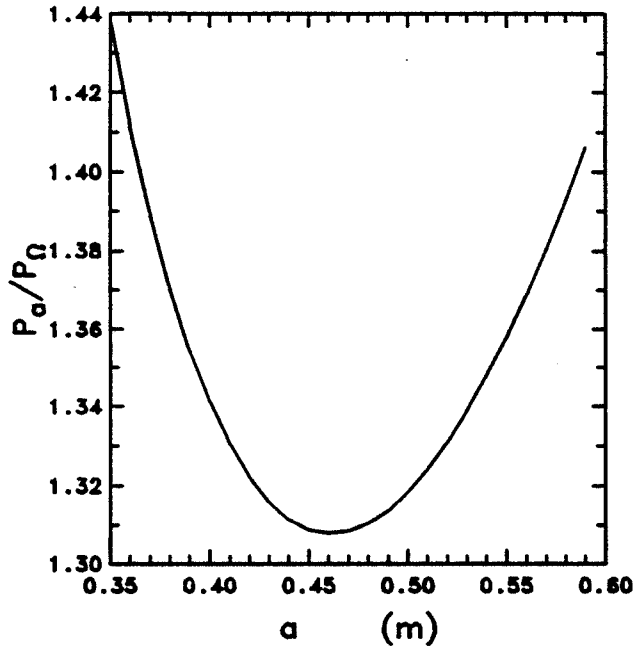


Figure 12: A plot of the quantity P_a/P_0 versus the minor radius a , and the total auxiliary power P_a versus a

By considering Goldston Scaling (see table 3 for the appropriate parameters) the function P_a/P_Ω is minimized with respect to N within a range of minor radii a . The minimum of the function P_a/P_Ω is plotted versus a in Fig. 12. Note that P_a/P_Ω has a well defined minimum at $a \sim 0.46m$. Also shown in Fig. 12 is a plot of the total amount of auxiliary power required at ignition versus a . Note that at the optimum minor radius the required auxiliary power is 2.4 MW. This small amount of auxiliary power required for ignition may now be viewed as a justification for choosing to minimize the quantity P_a/P_Ω .

Other important parameters characterizing the design are the the major radius (R), the toroidal magnetic field on axis (B), and the plasma current (I). These parameters are shown in Fig. 13 as a function of the minor radius a . Also shown on Fig. 13 is the parameter $B\tau/R$ as a function of minor radius.

Earlier work by Cohn[11,12] has also suggested the possible advantage of tokamak designs characterized by high magnetic fields. In particular Cohn's work has shown the advantage of designs characterized by high values of the parameter B^2a . Usually for $B^2a \geq 150$ ohmic ignition is possible thereby minimizing the adverse effect of auxiliary power on machine performance. The parameters $B\tau_E/R$ and B^2a are equivalent for the case of Neo-Alcator scaling and for operation under a fixed Murakami parameter nR/B .

The plasma current I decreases from 10 MA at $a = 0.6m$ to 7 MA at the optimum $a = 0.46m$. This decrease is a consequence of the decrease in the plasma minor radius a . Note that, even though the total plasma current is low at the optimum design point, the designs should not be considered low current devices since q_* has been set at the MHD stability limit ($q_* = 2$).

In Fig. 13 the parameter $W = B\tau_E/R$ is also plotted as a function of the plasma radius a . Note that the parameter $B\tau_E/R$ is maximized at the optimum radius a .

Similar results are obtained for other scalings. For the ITER scaling the optimum P_a/P_Ω and the corresponding major radius, plasma current,

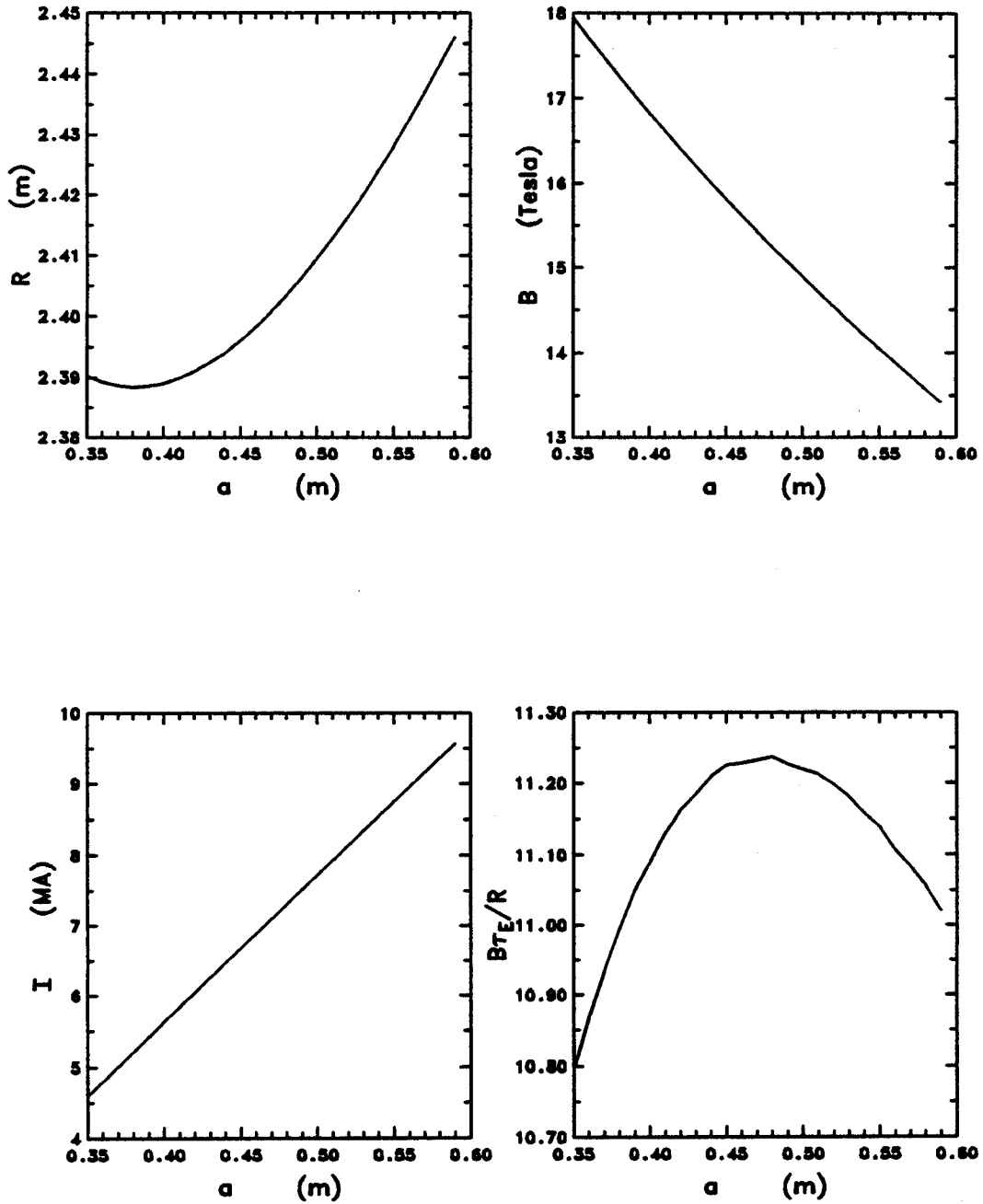


Figure 13: Clockwise from top are plotted the major radius R , the toroidal magnetic field B , the optimized performance parameter $B\tau_E/R$, and the plasma current I as a function of radius a

Table 4: Summary of the optimized design parameters for Goldston, Neo-Alcator, and ITER scalings

	Goldston	Neo-Alcator	ITER
a (m)	0.46	0.39	0.82
R (m)	2.4	2.39	2.58
R/a	5.2	6.0	3.1
B (T)	15.5	17.0	10.5
I (MA)	7.0	5.5	13.5
P_a (MW)	2.4	0.5	8.3
T_I (keV)	8.5	5.0	5.7
N_I	0.75	1.1	0.99
$B\tau_E/R$	11.2	21.5	6.83

and magnetic field are plotted on Fig. 14. Note again that there is a well defined minor radius a at which P_a/P_Ω is minimized. However, for the ITER scaling the optimum is obtained at a different point. On table 4 the parameters representing the optimized design for Goldston, Neo-Alcator, and ITER confinement scalings are summarized.

6 Conclusions

The volume averaged plasma power balance gives the characteristics of the global plasma behavior. Since the transport of heat is governed by the global energy confinement time τ_E , and because of the large number of scaling relations for τ_E there is no agreement on the choice of an appropriate parameter which can represent the plasma performance. In this chapter it was shown that by introducing the parameters W , Π , and N the behavior of the plasma can be characterized within a small range of W . In general $W \sim 15$ is required for ohmic ignition regardless of the type of confinement scaling. Also values of W less than 5 are not desirable since the auxiliary power required for ignition at these low values of W become very large.

Next by minimizing the parameter P_a/P_Ω optimized and ignited designs are obtained. By minimizing the ratio of auxiliary power to ohmic power,

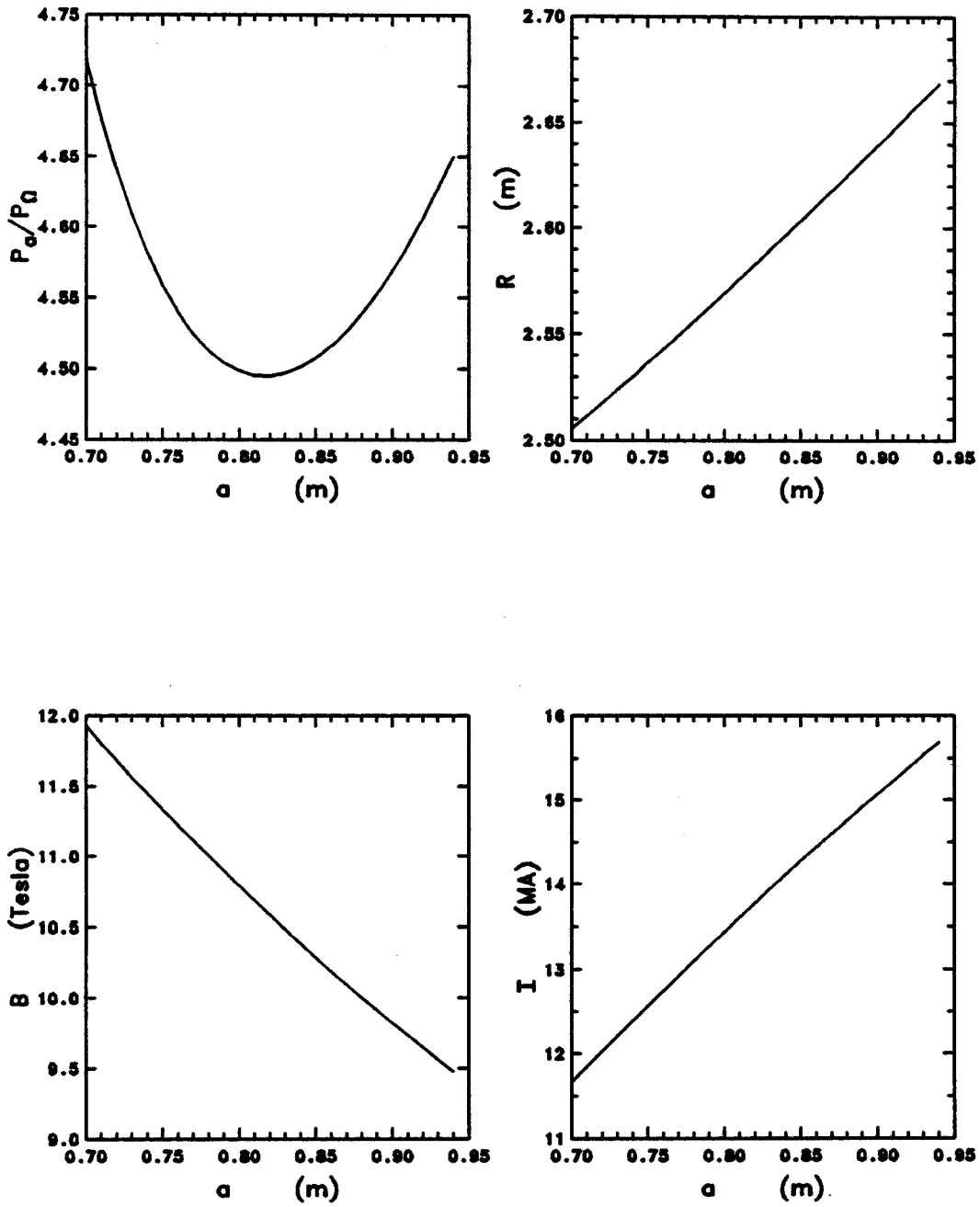


Figure 14: Clockwise from top left: The optimized parameter P_a/P_0 , the major radius, the plasma current, and the magnetic field as a function of plasma minor radius corresponding to ITER scaling

subject to a constraint of fixed toroidal field coil volume, designs are obtained for various forms of the parameter W . For Goldston and Neo-Alcator type confinement scalings, designs were obtained indicating the possible advantage of high aspect ratio and high magnetic fields. In particular the optimization results in geometries with aspect ratio ~ 5 and with toroidal magnetic fields in the order of 15 Tesla. These designs are further characterized by low total plasma currents while the required auxiliary power is also small. Optimization under ITER scaling results in configurations with lower aspect ratio and thus lower toroidal magnetic field.

APPENDIX A

$$\begin{aligned}
 F_{\alpha}(T) &= \frac{10^{22}}{T^{(2\nu_n+1)/\nu_T}} \int_0^T \sigma v(\xi) \xi^{\frac{2\nu_n+1}{\nu_i}-1} d\xi \\
 C_{\Omega} &= 0.3479 \frac{1 + \nu_n + \nu_T}{1 + 1.5\nu_T} \left(\frac{1 + \kappa^2}{\kappa} \right)^2 Z_{eff} \\
 C_{\alpha} &= 2.9167 \frac{1 + \nu_n + \nu_T}{\nu_T} \\
 C_b &= 0.1104 \frac{1 + \nu_n + \nu_T}{1 + 2\nu_n + .5\nu_T} Z_{eff} \\
 C_a &= 1.0563 \frac{1 + \nu_n + \nu_T}{\kappa}
 \end{aligned}$$

ν_n , and ν_T are parameters which determine the shape of the density and temperature profiles. In the calculations presented $\nu_n = \nu_T = 1$. σv is given in m^3/sec .

subject to a constraint of fixed toroidal field coil volume, designs are obtained for various forms of the parameter W . For Goldston and Neo-Alcator type confinement scalings, designs were obtained indicating the possible advantage of high aspect ratio and high magnetic fields. In particular the optimization results in geometries with aspect ratio ~ 5 and with toroidal magnetic fields in the order of 15 Tesla. These designs are further characterized by low total plasma currents while the required auxiliary power is also small. Optimization under ITER scaling results in configurations with lower aspect ratio and thus lower toroidal magnetic field.

APPENDIX A

$$\begin{aligned}
 F_{\alpha}(T) &= \frac{10^{22}}{T^{(2\nu_n+1)/\nu_T}} \int_0^T \sigma v(\xi) \xi^{\frac{2\nu_n+1}{\nu_n}-1} d\xi \\
 C_{\Omega} &= 0.3479 \frac{1 + \nu_n + \nu_T}{1 + 1.5\nu_T} \left(\frac{1 + \kappa^2}{\kappa} \right)^2 Z_{eff} \\
 C_{\alpha} &= 2.9167 \frac{1 + \nu_n + \nu_T}{\nu_T} \\
 C_b &= 0.1104 \frac{1 + \nu_n + \nu_T}{1 + 2\nu_n + .5\nu_T} Z_{eff} \\
 C_a &= 1.0563 \frac{1 + \nu_n + \nu_T}{\kappa}
 \end{aligned}$$

ν_n , and ν_T are parameters which determine the shape of the density and temperature profiles. In the calculations presented $\nu_n = \nu_T = 1$. σv is given in m^3/sec .

References

- [1] F. Troyon et al. MHD limits to plasma confinement. *Plasma physics and controlled fusion*, 26:209, 1984.
- [2] F. Troyon and R. Gruber. A semi-empirical scaling law for the β limit in tokamaks. *Physics Letters*, 29:110, 1985.
- [3] M. Murakami et al. Some Observations on Maximum Density in Tokamak Experiments. *Nuclear Fusion*, 16(2), 1976.
- [4] I.H. Hutchinson. Requirements for Ohmic Ignition. *Journal of Fusion Energy*, 6(3), 1987.
- [5] W.A Houlberg, S.E Attenberger, and S.M. Hively. *Nuclear Fusion*, 2:935-945, 1982.
- [6] E.A. Chaniotakis. *Ignition and Burn Control Characteristics of Thermonuclear Plasmas*. PhD thesis, Massachusetts Institute of Technology, 1990.
- [7] L. Bromberg. Private Communication.
- [8] J.A. Stratton. *Electromagnetic Theory*. McGraw-Hill, New York, 1941.
- [9] B. D. Montgomery. *Solenoid Magnet Design*. Robert E. Krieger Publishing Company, Huntington New York, 1980.
- [10] ITER Physics Design Guidelines. Technical report, IAEA, Vienna, 1990.
- [11] D.R. Cohn and L. Bromberg. *Journal of Fusion Energy*, 5:161, 1986.
- [12] D.R. Cohn. *Journal of Fusion Energy*, 6:281, 1987.